Inorg. Chem. **2009**, *48*, 915−924

Self-Assembly of a Series of Cobalt(II) Coordination Polymers Constructed from H_2tbip and Dipyridyl-Based Ligands

Lu-Fang Ma,[†] Li-Ya Wang,*[,†] Yao-Yu Wang,[‡] Stuart R. Batten,*[,§] and Jian-Ge Wang[†]

College of Chemistry and Chemical Engineering, Luoyang Normal University, Luoyang 471022, P. R. China, Key Laboratory of Synthetic and Natural Functional Molecule Chemistry of Ministry of Education, Department of Chemistry, Northwest University, Xi'an 710069, P. R. China, and School of Chemistry, Monash University, Victoria 3800, Australia

Received July 10, 2008

A series of interesting Co(II)−H_2tbip coordination polymers incorporating different auxiliary ligands, $\{[Co(tbip)(bipy)(H_2O)_3]\cdot 0.5(bipy)\cdot H_2O\}_n$ (**1**), $[Co(tbip)(bipy)]_n$ (**2**), $\{[Co_3(tbip)_3(dpe)_3]\cdot 0.5(dpe)\cdot 3H_2O\}_n$ (**3**), $[Co_2(tbip)_2(dpe)(H_2O)]_n$ (**4**), $[Co_2(tbip)_2(bpa)(H_2O)]_n$ (**5**), and $\{[Co_2(tbip)_2(bpa)_2]\cdot 2.5H_2O\}_n$ (**6**) (H_2tbip = 5-*tert*-butyl isophthalic acid; bipy = 4,4′-bipyridine; dpe = 1,2-di (4-pyridyl)ethylene; bpa = 1,2-bi(4-pyridyl)ethane) were synthesized. X-ray structural analyses of **1**−**6** reveal a diverse range of structures, ranging from 1D (**1**) to 2D (**2**, **6**) to 3D (**3**, **4**, **5**). Complex **1** shows 1D zigzag bipy-bridged polymeric chains with the terminal tbip ligands as pendants, which are extended to a 3D hydrogen-bonded supramolecular framework involving 1D open channels which encapsulate guest bipy molecules. Polymers **2** and **6** feature similar 2D infinite layer frameworks consisting of cobalt dimers. The structure of **3** is constructed from $[Co_2(tbip)_2]_n$ layers, which consists of alternating left- and right-handed helical chains, and further pillared by dpe ligands into a 3D six-connected self-penetrating $4^8.6^6.8$ network. The prominent cavities in **3** are parallel to the (101) plane and encapsulate free dpe as guest molecules. Polymers **4** and **5** are isostructural, showing 2-fold interpenetrating 3D α-Po networks constructed from binuclear cobalt nodes. The thermal stabilities and X-ray powder diffraction studies indicate that the framework of **3** can keep stable after the loss of guest molecules. Studies of the magnetic susceptibilities of **2**−**6** reveal weak antiferromagnetic exchange interactions between adjacent Co(II) centers.

Introduction

The design and synthesis of metal-organic frameworks based on the selection of ligands and metal ions has become a very attractive research field. The motive comes not only from the intriguing structural diversity but also from the demand for applications of functional materials in the fields of catalysis, porosity, magnetism, luminescence, conductivity, sensing, nonlinear optics, and chirality.[1−6] One of the obvious challenges is the rational and controllable preparation of metal-organic frameworks, the formation of which is greatly affected by the organic ligands, the nature of the metal ions, the counterions, and other factors. Among the reported studies, organic ligands with carboxylate groups are especially interesting because they can adopt a variety of coordination modes and result in diverse multidimensional architectures.[7−10] However, most of the reported work has

* To whom correspondence should be addressed. E-mail: wlya@lynu.edu.cn (L.-Y.W.).
† Luoyang Normal University.
‡ Northwest University.
§ Monash University.

(1) (a) Sun, D.; Ma, S.; Ke, Y.; Collins, D. J.; Zhou, H. C. *J. Am. Chem. Soc.* **2006**, *128*, 3896. (b) Khlobystov, A. N.; Blake, A. J.; Champness, N. R.; Lemenovskii, D. A.; Majouga, A. G.; Zyk, N. V.; Schröder, M. *Coord. Chem. Rev.* **2001**, *222*, 155. (c) Eddaoudi, M.; Moler, D. B.; Li, H. L.; Chen, B. L.; Reineke, T. M.; O'Keeffe, M.; Yaghi, O. M. *Acc. Chem. Res.* **2001**, *34*, 319. (d) Yaghi, O. M.; O'Keeffe, M.; Ockwig, N. W.; Chae, H. K.; Eddaoudi, M.; Kim, J. *Nature* **2003**, *423*, 705. (e) Férey, G.; Mellot-Draznieks, C.; Serre, C.; Millange, F. *Acc. Chem. Res.* **2005**, *38*, 217. (f) Gao, X. M.; Li, D. S.; Wang, J. J.; Fu, F.; Wu, Y. P.; Hu, H. M.; Wang, J. W. *CrystEngComm* **2008**, *10*, 479.

(2) (a) Rowsell, J. L. C.; Yaghi, O. M. *J. Am. Chem. Soc.* **2006**, *128*, 1304. (b) Latroche, M.; Surble, S.; Serre, C.; Mellot-Draznieks, C.; Llewellyn, P. L.; Lee, J. H.; Chang, J. S.; Jhung, S. H.; Ferey, G. *Angew. Chem., Int. Ed.* **2006**, *45*, 8227. (c) Zeng, M. H.; Wang, B.; Wang, X. Y.; Zhang, W. X.; Chen, X. M.; Gao, S. *Inorg. Chem.* **2006**, *45*, 7069. (d) Tang, Y. Z.; Huang, X. F.; Song, Y. M.; Hong Chan, P. W.; Xiong, R. G. *Inorg. Chem.* **2006**, *45*, 4868. (e) Verbiest, T.; van Elshocht, S.; Karuanen, M.; Hellemans, L.; Snauwaert, J.; Nuckolls, C.; Katz, T. J.; Persoons, A. *Science* **1998**, *282*, 913.

10.1021/ic801278j CCC: $40.75
Published on Web 12/31/2008

been devoted to the use of 1,3-benzenedicarboxylic acid, 1,3,5-benzenetricarboxylic acid, 1,2,4,5-benzenetetracarboxylic acid, and so on, while the use of the large steric hindrance of the H_2tbip ligand remains largely unexplored. To the best of our knowledge, there has been only one reported polymer based on the H_2tbip ligand hitherto.[11] The presence of the electron-donating ($-C(CH_3)_3$) noncoordinating groups in dicarboxylate ligands changes their electronic and steric properties, which can generate complexes different from those of the common dicarboxylate ligands.

On the other hand, rodlike *N*,*N*′-donor building blocks, such as the conventionally employed 4,4′-bipyridine, have been extensively studied in coordination chemistry, and modification by introducing spacers between the two 4-pyridyl groups can result in distinct spatial effects to produce unexpected architectures with metal complexes. The use of these auxiliary ligands may contribute to an understanding of the assembly and recognition processes in coordination chemistry.[12,13] Therefore, systematic studies have been carried out in our laboratory by the reaction of Co(II) salts, the H_2tbip ligand, and a series of N-donor ligands to investigate the influence of multicarboxylate and N-donor ligands on the properties and construction of coordination frameworks, and six novel Co(II) coordination polymers, $\{[Co(tbip)(bipy)(H_2O)_3]\cdot 0.5(bipy)\cdot H_2O\}_n$ (**1**), $[Co(tbip)(bipy)]_n$ (**2**), $\{[Co_3(tbip)_3(dpe)_3]\cdot 0.5(dpe)\cdot 3H_2O\}_n$ (**3**), $[Co_2(tbip)_2(dpe)(H_2O)]_n$ (**4**), $[Co_2(tbip)_2(bpa)(H_2O)]_n$ (**5**), and $\{[Co_2(tbip)_2(bpa)_2]\cdot 2.5\ H_2O\}_n$ (**6**), were successfully obtained by tuning the reaction conditions including the pH value, reaction temperature, and auxiliary ligand. They exhibit diverse structures with dimensionalities from 1D to 3D, of which **1** shows a 1D zigzag chain, **2** and **6** exhibit a 2D layer motif, **3** displays a 3D self-penetrating framework, and interestingly **4** and **5** possess 2-fold interpenetrating 3D α-Po networks. The details of their syntheses, structures, and magnetic properties are reported below (see also Scheme 1).

Scheme 1. Coordination Modes of H_2tbip Observed in **1**−**6**

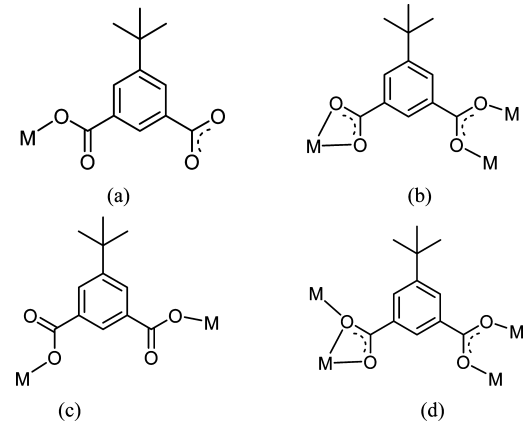

Experimental Section

Materials and Physical Measurements. All reagents used in the syntheses were of analytical grade. Elemental analyses for carbon, hydrogen, and nitrogen atoms were performed on a Vario EL III elemental analyzer. The infrared spectra (4000∼400 cm^{-1}) were recorded by using KBr pellets on an Avatar 360 E.S.P. IR spectrometer. Thermogravimetric analyses (TG) were carried out on a STA449C integration thermal analyzer. The powder X-ray diffraction (PXRD) patterns were recorded with a Rigaku D/Max

(3) (a) Hagrman, P. J.; Hagrman, D.; Zubieta, J. *Angew. Chem., Int. Ed.* **1999**, *38*, 2638. (b) Chen, B.; Ma, S.; Zapata, F.; Fronczek, F. R.; Lobkovsky, E. B.; Zhou, H. C. *Inorg. Chem.* **2007**, *46*, 1233. (c) Moulton, B.; Zaworotko, M. J. *Chem. Rev.* **2001**, *101*, 1629.
(4) (a) Dinca, M.; Long, J. R. *J. Am. Chem. Soc.* **2005**, *127*, 9376. (b) Chen, B. L.; Ockwig, N. W.; Millward, A. R.; Contreras, D. S.; Yaghi, O. M. *Angew. Chem., Int. Ed.* **2005**, *44*, 4745. (c) Kesanli, B.; Lin, W. *Coord. Chem. Rev.* **2003**, *246*, 305. (d) Barbour, L. J. *Chem. Commun.* **2006**, 1163. (e) Horike, S.; Matsuda, R.; Tanaka, D.; Mizuno, M.; Endo, K.; Kitagawa, S. *J. Am. Chem. Soc.* **2006**, *128*, 4222.
(5) (a) Ma, L. F.; Wang, L. Y.; Huo, X. K.; Wang, Y. Y.; Fan, Y. T.; Wang, J. G.; Chen, S. H. *Cryst. Growth Des.* **2008**, *8*, 620. (b) Ma, L. F.; Wang, Y. Y.; Wang, L. Y.; Liu, J. Q.; Wu, Y. P.; Wang, J. G.; Shi, Q. Z.; Peng, S. M. *Eur. J. Inorg. Chem.* **2008**, 693. (c) Ma, L. F.; Huo, X. K.; Wang, L. Y.; Fan, Y. T.; Wang, J. G. *J. Solid State Chem.* **2007**, *180*, 1648.
(6) (a) Yang, J.; Yue, Q.; Li, G. D.; Cao, J. J.; Li, G. H.; Chen, J. S. *Inorg. Chem.* **2006**, *45*, 2857. (b) Yue, Q.; Yang, J.; Li, G. H.; Li, G. D.; Xu, W.; Chen, J. S.; Wang, S. N. *Inorg. Chem.* **2005**, *44*, 5241. (c) Ma, B. Q.; Zhang, D. S.; Gao, S.; Jin, T. Z.; Yan., C. H. *Angew. Chem., Int. Ed.* **2000**, *39*, 3644.
(7) (a) Zhao, B.; Cheng, P.; Chen, X. Y.; Cai, C.; Wei, S.; Liao, D. Z.; Yan, S. P.; Jiang, Z. H. *J. Am. Chem. Soc.* **2004**, *126*, 3012. (b) Chun, H.; Dybtsev, D. N.; Kim, H.; Kim, K. *Chem.—Eur. J.* **2005**, *11*, 3521. (c) Sun, D. F.; Cao, R.; Liang, Y. C.; Shi, Q.; Hong, M. C. *Dalton Trans.* **2002**, 1847. (d) Zhao, B.; Cheng, P.; Dai, Y.; Cheng, C.; Liao, D. Z.; Yan, S. P.; Jiang, Z. H.; Wang, G. L. *Angew. Chem., Int. Ed.* **2003**, *42*, 934. (e) Li, X. J.; Cao, R.; Bi, W. H.; Wang, Y. Q.; Wang, Y. L.; Li, X. *Polyhedron* **2005**, *24*, 2955. (f) Lin, J. G.; Zang, S. Q.; Tian, Z. F.; Li, Y. Z.; Xu, Y. Y.; Zhu, H. Z.; Meng, Q. J. *CrystEngComm.* **2007**, *9*, 915. (g) Liu, Q. Y.; Yuan, D. Q.; Xu, L. *Cryst. Growth Des.* **2007**, *7*, 1832.
(8) (a) Liang, Y. C.; Cao, R.; Su, W. P.; Hong, M. C.; Zhang, W. J. *Angew. Chem., Int. Ed.* **2000**, *39*, 3304. (b) Pan, L.; Huang, X. Y.; Li, J.; Wu, Y. G.; Zheng, N. W. *Angew. Chem., Int. Ed.* **2000**, *39*, 527. (c) Du, M.; Jiang, X. J.; Zhao, X. J. *Chem. Commun.* **2005**, 5521. (d) Ohmura, T.; Mori, W.; Hasegawa, M.; Takei, T.; Yoshizawa, A. *Chem. Lett.* **2003**, *32*, 34. (e) Kesanli, B.; Cui, Y.; Smith, M. R.; Bittner, E. W.; Bockrath, B. C.; Lin, W. B. *Angew. Chem., Int. Ed.* **2005**, *44*, 72. (f) Pan, L.; Frydel, T.; Sander, M. B.; Huang, X. Y.; Li, J. *Inorg. Chem.* **2001**, *40*, 1271.
(9) (a) Bickley, J. F.; Bonar-Law, R. P.; Femoni, C.; MacLean, E. J.; Steiner, A.; Teat, S. J. *Dalton Trans.* **2000**, 4025. (b) Zhang, X. M.; Tong, M. L.; Chen, X. M. *Angew. Chem., Int. Ed.* **2002**, *41*, 1029. (c) Kirillov, M.; Kopylovich, M. N.; Kirillova, M. V.; Haukka, M.; Guedes da Silva, M. F. C.; Pombeiro, A. J. L. *Angew. Chem., Int. Ed.* **2005**, *44*, 4345. (d) Barthelet, K.; Riou, D.; Nogues, M.; Ferey, G. *Inorg. Chem.* **2003**, *42*, 1739. (e) Ma, A. Q.; Shi, Z.; Xu, R. R.; Pang, W. Q.; Zhu, L. G. *Chem. Lett.* **2003**, *32*, 1010.
(10) (a) Xiao, D. R.; Wang, E. B.; An, H. Y.; Su, Z. M.; Li, Y. G.; Gao, L.; Sun, C. Y.; Xu, L. *Chem.—Eur. J.* **2005**, *11*, 6673. (b) Liang, Y. C.; Hong, M. C.; Su, W. P.; Cao, R.; Zhang, W. J. *Inorg. Chem.* **2001**, *40*, 4574. (c) Shi, X.; Zhu, G. S.; Wang, X. H.; Li, G. H.; Fang, Q. R.; Wu, G.; Ge, T.; Xue, M.; Zhao, X. J.; Wang, R. W.; Qiu, S. L. *Cryst. Growth Des.* **2005**, *5*, 207. (d) Liu, C. S.; Wang, J. J.; Yan, L. F.; Chang, Z.; Bu, X. H.; Sanudo, E. C.; Ribas, J. *Inorg. Chem.* **2007**, *46*, 6299. (e) Gu, X. J.; Xue, D. F. *CrystEngComm.* **2007**, *9*, 471.
(11) Pan, L.; Parker, B.; Huang, X. Y.; Oison, D. H.; Lee, J. Y.; Li, J. *J. Am. Chem. Soc.* **2006**, *128*, 4180.
(12) (a) Eddaoudi, M.; Kim, J.; Rosi, N.; Vodak, D.; Wachter, J.; O'Keeffe, M.; Yaghi, O. M. *Science* **2002**, *295*, 469. (b) Sharma, C. V. K.; Rogers, R. D. *Chem. Commun.* **1999**, 83. (c) Wang, Q. M.; Guo, G. C.; Mak, T. C. W. *Chem. Commun.* **1999**, 1849. (d) Wang, C. C.; Yang, C. H.; Tseng, S. M.; Lee, G. H.; Chiang, Y. P.; Sheu, H. S. *Inorg. Chem.* **2003**, *42*, 8294. (e) Wang, C. C.; Lin, H. W.; Yang, C. H.; Liao, C. H.; Lan, I. T.; Lee, G. H. *New J. Chem.* **2004**, *28*, 180. (f) Zhuang, W. J.; Zheng, X. J.; Li, L. C.; Liao, D. Z.; Ma, H.; Jin, L. P. *CrystEngComm.* **2007**, *9*, 653.
(13) (a) Noro, S.; Kitaura, R.; Kondo, M.; Kitagawa, S.; Ishii, T.; Matsuzaka, H.; Yamashita, M. *J. Am. Chem. Soc.* **2002**, *124*, 2568. (b) Hennigar, T. L.; MacQuarrie, D. C.; Losier, P.; Rogers, R. D.; Zaworotko, M. J. *Angew. Chem., Int. Ed. Engl.* **1997**, *36*, 972. (c) Carlucci, L.; Ciani, G.; Macchi, P.; Proserpio, D. M. *Chem. Commun.* **1998**, 1837. (d) Huang, X. C.; Zhang, J. P.; Lin, Y. Y.; Yu, X. L.; Chen, X. M. *Chem. Commun.* **2004**, 1100.

Table 1. Crystallographic Data for Complexes **1**−**6**

	1	**2**	**3**	**4**	**5**	**6**
formula	$C_{27}H_{32}CoN_3O_8$	$C_{22}H_{20}CoN_2O_4$	$C_{78}H_{77}Co_3N_7O_{15}$	$C_{36}H_{36}Co_2N_2O_9$	$C_{36}H_{38}$ $Co_2N_2O_9$	$C_{48}H_{53}Co_2N_4O_{10.5}$
fw	585.49	435.33	1529.3	758.53	760.54	971.80
temperature	291(2)	296(2)	291(2)	291(2)	291(2)	293(2)
cryst syst	triclinic	monoclinic	monoclinic	monoclinic	monoclinic	triclinic
space group	$P\bar{1}$	$C2/m$	$C2/c$	$P2_1/n$	$P2_1/n$	$P\bar{1}$
unit cell dimensions (Å, deg)	a = 8.1028(2)	a = 21.690(3)	a = 23.8309(11)	a = 9.5735(13))	a = 9.5846(9)	a = 10.1485(11)
	b = 11.037(2)	b = 11.399(14)	b = 13.3997(6)	b = 17.493(2)	b = 17.5051(17)	b = 11.6152(13)
	c = 16.541(4)	c = 9.9980(12)	c = 46.339(2)	c = 21.188(3)	c = 21.321(2)	c = 23.006(3)
	α = 107.126(2)					α =76.6490(10)
	β = 103.022(2)	β = 102.578(10)	β = 98.8(10)	β = 102.191(2)	β = 101.7560(10)	β = 77.8030(10)
	γ = 91.105(3)					γ = 74.0840(10)
V(Å^3)	1371.5(5)	2412.6(5)	14623.0(12)	3468.2(8)	3502.2(6)	2505.5(5)
Z	2	4	8	4	4	2
ρ (g cm^{-3})	1.418	1.198	1.389	1.453	1.442	1.288
F(000)	612	900	6360	1568	1576	1014
GOF	1.049	1.089	1.080	1.026	1.025	1.046
R_1,wR_2 [$I > 2\sigma$ (I)]	0.0452,0.1082	0.0813, 0.2611	0.0527, 0.1362	0.0275, 0.0665	0.0251, 0.0649	0.0663, 0.1997
R_1,wR_2 (all data)	0.0666, 0.1194	0.0878, 0.2704	0.0728, 0.1476	0.0350, 0.0705	0.0282, 0.0669	0.1063, 0.2318
residuals (e Å^{-3})	0.460, −0.326	1.196, −0.928	0.533, −0.665	0.265, −0.375	0.338, −0.309	1.122, −0.750

3III diffractometer. Variable-temperature magnetic susceptibilities were measured using a MPMS-7 SQUID magnetometer. Diamagnetic corrections were made with Pascal's constants for all constituent atoms.

Synthesis of {[Co(tbip)(bipy)(H_2O)$_3$]·0.5(bipy)·H_2O}$_n$ (1). A mixture of 5-*tert*-butyl isophthalic acid (0.1 mmol, 23.1 mg), bipy (0.1 mmol, 15.9 mg), $Co(OAc)_2·4H_2O$ (0.05 mmol, 12.0 mg), NaOH (0.1 mmol, 4.0 mg), and H_2O (15 mL) was placed in a Teflon-lined stainless steel vessel, heated to 120 °C for 3 days, and then cooled to room temperature over 24 h. Red block crystals of **1** were obtained. Elem anal. (%) calcd for $C_{27}H_{32}CoN_3O_8$: C, 55.39; H, 5.51; N, 7.18. Found: C, 55.48; H, 5.39; N, 7.12. IR (cm^{-1}): 3437 m, 2926 m, 1609 s, 1558 m, 1371 s, 823 w, 545 m.

Synthesis of [Co(tbip)(bipy)]$_n$ (2). The synthesis was similar to that described for **1**, except that 0.2 mmol of NaOH was used instead of 0.1 mmol of NaOH. Pink crystals of **2** were obtained. Elem anal. (%) calcd for $C_{22}H_{20}CoN_2O_4$: C, 60.70; H, 4.63; N, 6.43. Found: C, 60.78; H, 4.56; N, 6.32. IR (cm^{-1}): 3400 m, 2964 m, 1685 s, 1606 m, 1550 m, 1367 m, 759 m, 631 m.

Synthesis of {[Co_3(tbip)$_3$(dpe)$_3$]·0.5(dpe)·3H_2O}$_n$ (3). A mixture of 5-*tert*-butyl isophthalic acid (0.1 mmol, 23.1 mg), 1,2-di(4-pyridyl)ethylene (0.1 mmol, 18.1 mg), $Co(OAc)_2·4H_2O$ (0.05 mmol, 12.0 mg), NaOH (0.2 mmol, 8.0 mg), and H_2O (15 mL) was placed in a Teflon-lined stainless steel vessel, heated to 120 °C for 3 days, and then cooled to room temperature over 24 h. Dark red block crystals of **3** were obtained. Elem anal. (%) calcd for $C_{78}H_{77}Co_3N_7O_{15}$: C, 61.26; H, 5.07; N, 6.41. Found: C, 61.39; H, 5.09; N, 6.31. IR (cm^{-1}): 3455 m, 2959 m, 1608 s, 1569 m, 1433 m, 1368 m, 779 m, 723 m.

Synthesis of [Co_2(tbip)$_2$(dpe)(H_2O)]$_n$ (4). The synthesis was similar to that described for **3** except that the reaction mixture was heated at 160 °C. Red crystals of **4** were obtained. Elem anal. (%) calcd for $C_{36}H_{36}Co_2N_2O_9$: C, 57.00; H, 4.78; N, 3.69. Found: C, 57.08; H, 4.71; N, 3.62. IR (cm^{-1}): 3443 m, 2965 m, 1624 s, 1609 s, 1561 m, 1437 m, 1385 m, 827 m, 714 m, 552 m.

Synthesis of [Co_2(tbip)$_2$(bpa)(H_2O)]$_n$ (5). The synthesis was similar to that described for **4** except that 1,2-di(4-pyridyl)ethylene was replaced by 1,2-bis(4-pyridyl)ethane. Red crystals of **5** were obtained. Elem anal. (%) calcd for $C_{36}H_{38}Co_2N_2O_9$: C, 56.85; H, 5.04; N, 3.68. Found: C, 56.79; H, 5.01; N, 3.74. IR (cm^{-1}): 3381 m, 2963 m, 1613 s, 1571 s, 1432 m, 1368 m, 830 m, 721 m, 551 m.

Synthesis of {[Co_2(tbip)$_2$(bpa)$_2$]·2.5H_2O}$_n$ (6). The synthesis was similar to that described for **3** except that 1,2-di(4-pyridyl)-ethylene was replaced by 1,2-bis(4-pyridyl)ethane. Red crystals of **6** were obtained. Elem anal. (%) calcd for $C_{48}H_{53}Co_2N_4O_{10.5}$: C, 59.32; H, 5.50; N, 5.77. Found: C, 59.21; H, 5.54; N, 5.69. IR (cm^{-1}): 3452 m, 2981 m, 1656 s, 1470 w, 1446 m, 1381s, 821 m, 732 m.

X-Ray Crystallography. Single-crystal X-ray diffraction analyses of **1**−**6** were carried out on a Bruker SMART APEX II CCD diffractometer equipped with graphite monochromated Mo Kα radiation (λ = 0.71073 Å) by using the ϕ/ω scan technique at room temperature. The structures were solved by direct methods with SHELXS-97. The hydrogen atoms were assigned with common isotropic displacement factors and were included in the final refinement by use of geometrical constraints. A full-matrix least-squares refinement on F^2 was carried out using SHELXL-97. The crystallographic data and selected bond lengths and angles for **1**−**6** are listed in Table 1 and Tables S1−S6, Supporting Information. Crystallographic data for the structural analysis have been deposited with the Cambridge Crystallographic Data Center. CCDC reference numbers: 694013−694018.

Results and Discussion

Hydrothermal Synthesis. Because the mixing of metal salts and carboxylate solutions usually results in precipitation in traditional aqueous reactions, making it difficult to grow crystals of complexes, hydrothermal methods were adopted in our studies, and these methods were proven to be a powerful approach for the preparation of sparingly soluble organic−inorganic hybrid materials.[14] As is known, there are a variety of hydrothermal parameters such as reaction time, temperature, pH value, template, and molar ratio of the reactants, and small changes in one or more of the parameters can have a profound influence on the final reaction outcome.[15,16] Our synthetic strategy for the Co(II)−H_2tbip coordination polymers is schematically de-

(14) (a) Tao, J.; Tong, M. L.; Shi, F. X.; Chen, X. M.; Ng, S. W. *Chem.Commun.* **2000**, 2043. (b) Feng, S.; Xu, R. *Acc. Chem. Res.* **2001**, *34*, 239. (c) Lu, J. Y. *Coord. Chem. Rev.* **2003**, *246*, 327.

(15) (a) Lin, Z. Z.; Jiang, F. L.; Chen, L.; Yuan, D. Q.; Zhou, Y. F.; Hong, M. C. *Eur. J. Inorg. Chem.* **2005**, 77. (b) Fang, R. Q.; Zhang, X. M. *Inorg. Chem.* **2006**, *45*, 4801. (c) Chen, W. X.; Wu, S. T.; Long, L. S.; Huang, R. B.; Zheng, L. S. *Cryst. Growth Des.* **2007**, *7*, 1171. (d) Huang, Y. Q.; Shen, Z. L.; Okamura, T.; Wang, Y.; Wang, X. F.; Sun, W. Y.; Yu, J. Q.; Ueyama, N. *Dalton Trans.* **2008**, 204. (e) Du, M.; Jiang, X. J.; Zhao, X. J. *Inorg. Chem.* **2006**, *45*, 3998.

Scheme 2. Synthesis of Complexes **1**−**6**

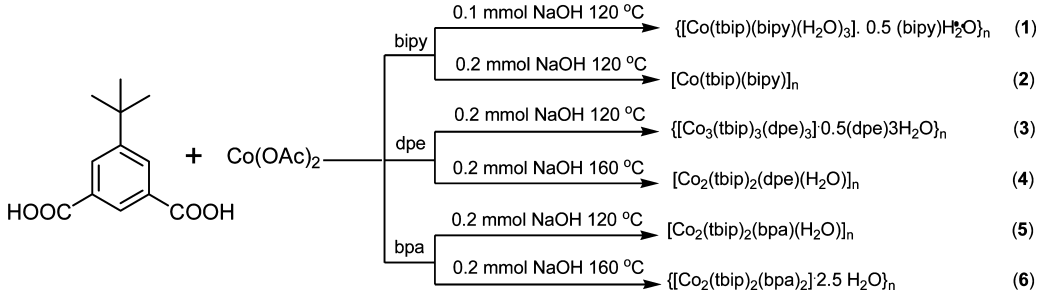

picted in Scheme 2. After many parallel experiments, it was found that complexes **1** and **2** were obtained under different pH values that were adjusted by the addition of NaOH. Compound **1** was the favored product with a relatively lower pH value (pH < 4), whereas compound **2** was the dominant product with a relatively higher pH value (pH > 5). Both novel 3D MOFs **3** and **4** were synthesized using the same reaction mixture but at different hydrothermal temperatures. The noninterpenetrating **3** was obtained at 120 °C, whereas the 2-fold interpenetrating **4** was formed at 160 °C, suggesting that the hydrothermal temperatures have a critical impact on the construction of 3D MOFs. It is noted that the change of hydrothermal temperatures to obtain interpenetrating and noninterpenetrating 3D MOFs has been reported rarely,[17] although several MOFs controlled by hydrothermal temperatures had been documented.[18] The successful isolation of **1**−**4** prompted us to extend our study to use flexible bpa instead of rigid bipy and dpe in **5** and **6**. A 2-fold interpenetrating **5** similar to **4** can be obtained, and a 2D layer framework was formed in **6**. Although detailed studies are still required to better understand the reason for the formation of the different types of structures, some similiar works have been documented previously.[7g]

Description of Crystal Structures. {[Co(tbip)(bipy)-(H_2O)$_3$]·0.5(bipy)·H_2O}$_n$ (1). X-ray analysis reveals that the asymmetric unit of **1** consists of one cobalt(II) cation, one monocoordinated tbip (Scheme 1a), one bridged bipy, three coordinated water molecules, and half an uncoordinated bipy as well as one free lattice water molecule. The coordination environment around the Co(II) ion can be described as a slightly distorted octahedron (as shown in Figure 1a). Each Co(II) ion is six-coordinated by two bipy nitrogen atoms, one carboxylic oxygen atom of tbip, and three lattice water O atoms. The Co−O bond lengths are in the range of 2.105(2)−2.155(2) Å, and the Co−N bond distances are 2.162(3) and 2.169(3) Å, respectively. As shown in Figure 1b, the bipy ligand acts as a μ_2-bridge and joins the Co atoms into an infinite 1D zigzag chain. The two pyridyl rings in a bipy ligand are almost coplanar. Multiple hydrogen bonds are known to cooperatively exert a dramatic influence on the control of molecular self-assembly in chemical and biological systems.[19] Here, in **1**, there exist extensive hydrogen-bonding interactions involving the tbip ligand as well as coordinated and free water molecules (Table S7, Supporting Information). Thus, a 3D

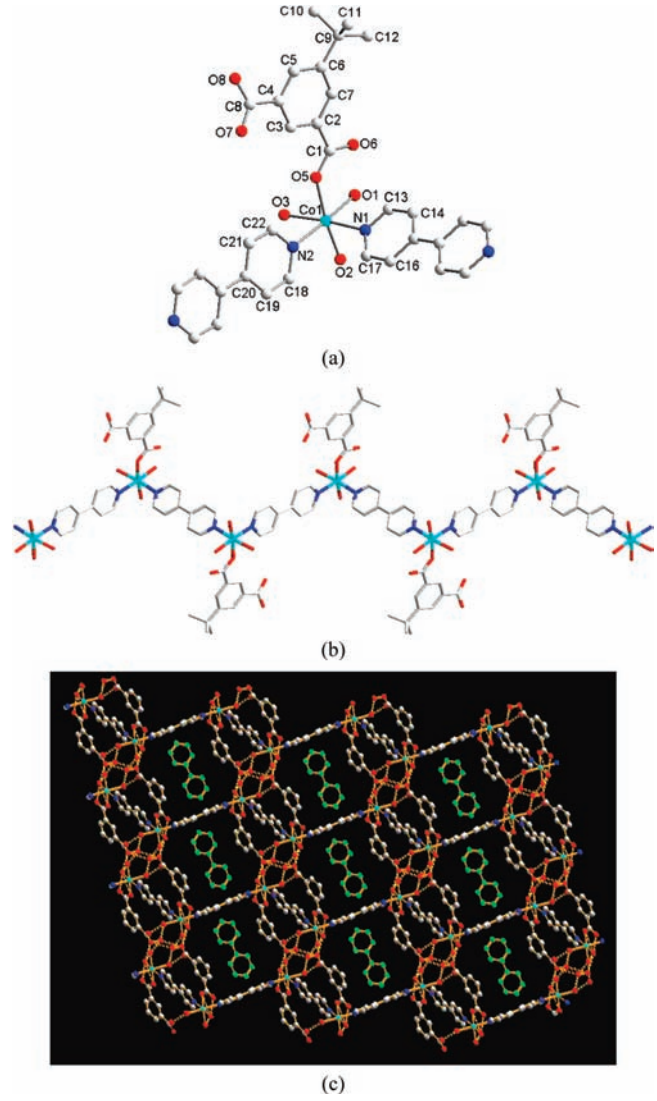

Figure 1. (a) Coordination environment of Co (II) ion in **1**. The hydrogen atoms, free bipy, and water are omitted for clarity. (b) View of the 1D zigzag chain bridged by bipy ligands. (c) A perspective view of the 3D network of compound **1** containing 1D open channels encapsulating bipy molecules. The hydrogen-bonding interactions are indicated by dashed lines.

(16) (a) Li, J. R.; Bu, X. H.; Zhang, R. H.; Ribas, J. *Cryst.Growth Des.* **2005**, *5*, 1919. (b) Zhang, X. J.; Zhou, X. P.; Li, D. *Cryst. Growth Des.* **2006**, *6*, 1440. (c) Wang, R. H.; Yuan, D. Q.; Jiang, F. L.; Han, L.; Gong, Y. Q.; Hong, M. C. *Cryst. Growth Des.* **2006**, *6*, 1351. (d) Ghosh, S. K.; Savitha, G.; Bharadwaj, P. K. *Inorg. Chem.* **2004**, *43*, 5497. (e) Fan, S. R.; Zhu, L. G. *Inorg. Chem.* **2006**, *45*, 7935.
(17) Liu, C. M.; Gao, S.; Zhang, D. Q.; Zhu, D. B. *Cryst. Growth Des.* **2007**, *7*, 1312.
(18) (a) Xue, X.; Wang, X. S.; Xiong, R. G.; You, X. Z.; Abrahams, B. F.; Che, C. M.; Ju, H. X. *Angew. Chem., Int. Ed.* **2002**, *41*, 2944. (b) Lee, L. S.; Shin, D. M.; Chung, Y. K. *Chem.—Eur. J.* **2004**, *10*, 3158.

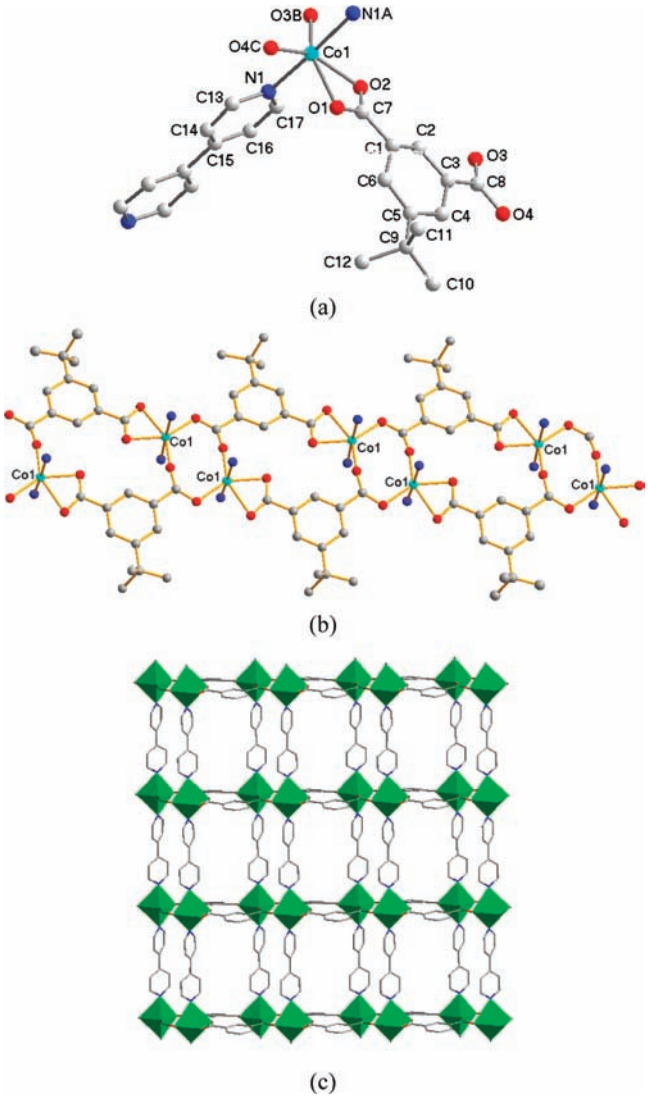

Figure 2. (a) Coordination environment of the Co(II) ion in **2**. The hydrogen atoms are omitted for clarity. (b) View of a 1D ribbonlike chain of Co atoms bridged by tbip ligands (c) Ribbonlike chains pillared by rigid bipy ligands into a 2D layer. The *tert*-butyl groups are ommitted for clarity.

supramolecular framework encapsulating guest bipy molecules is formed through these hydrogen bonds among the adjacent 1D chains. It is apparent that the formed 3D supramolecular structure is stabilized by free bipy molecules, which reside at the crossing positions of the tunnels (Figure 1c).

[Co(tbip)(bipy)]$_n$ (2). The asymmetric unit of **2** contains one Co^{2+} cation, one bipy ligand, and one tbip anion. As shown in Figure 2a, each Co atom is octahedrally coordinated by two nitrogen atoms of two bipy ligands and four oxygen atoms from three tbip ligands. The Co−$O_{(carboxylate)}$ and Co−$N_{(bipy)}$ bond lengths are in agreement with those in carboxylate- and bipy-containing cobalt(II) complexes. Each tbip anion acts as a tetradentate ligand in compound **2**, connecting three Co ions (Scheme 1b). Two carboxylic groups of the tbip ligand have two coordination modes, one bidentately bridging two Co atoms in a syn−syn fashion and the other chelating one Co atom. Along the (110) direction, the Co atoms are bridged by the tbip anions to generate 1D ribbonlike chains containing an alternative arrangement of 8- and 16-membered rings (Figure 2b). Two carboxylic groups bridge two Co(II) ions to form an eight-membered ring, and two tbip ligands bridge two Co(II) ions to form a 16-membered ring. Within the eight-membered ring and 16-membered ring, the Co···Co separations are 4.11 and 7.37 Å, respectively. The resulting chains are interlinked by the rigid bipy ligands to form a 2D layer (Figure 2c). Different from the coplanar bipy molecule in **1**, the bipy ligand is twisted with a dihedral angle of 26.7° between the two pyridyl components.

Interestingly, comparison of the structures of **1** and **2** with those of reported Co complexes constructed from 5-hydroxyl-1,3-benzenedicarboxylic acid (OH-BDC) and bipy,[20] {[Co(bipy)$(H_2O)_4$](OH-BDC)(H_2O)}$_n$ (**7**) and {[Co(bipy)(OH-BDC)$(H_2O)_2$](bipy)(DMF)}$_n$ (**8**), indicates some differences. First, the coordination modes of the carboxylate groups in polymers **1** and **2** are different from those of **7** and **8**: mono and tetradentate modes in **1** and **2** and noncoordinate and bis-monodentate modes in **7** and **8**. Second, compound **7** possesses hydrogen-bonded 3D networks encapsulating 1D linear covalently bonded infinite [Co(bipy)$(H_2O)_4]_n$ chains, and compound **8** shows a 2D architecture containing 1D strand chains bridged by OH−BDC. Both of the structures are different from those of **1** and **2**. Thus, although the carboxylic coordination sites of H_2tbip and OH−BDC are very similar, their coordination chemistries are obviously different, presumably due to the steric hindrance of the bulky *tert*-butyl skeleton.

{[Co_3(tbip)$_3$(dpe)$_3$]·0.5(dpe)·3H_2O}$_n$ (3). The crystal structure of **3** exhibits a 3D network composed of binuclear Co cluster nodes, dpe and tbip bridging ligands, free dpe, and water molecules. There are three crystallographic independent Co(II) ions in **3**. Each Co(II) ion adopts a distorted octahedral [O_4N_2] coordination geometry with four carboxylic oxygen atoms from three tbip ligands and two nitrogen atoms of two dpe ligands (Figure 3a). The Co−O and Co−N bond distances are in the ranges of 1.996(2)−2.246(3) and 2.133(3)−2.177(3) Å, respectively. The coordination mode of tbip in **3** is similar to that of **2** (Scheme 1b). As shown in Figure 3c and d, two Co centers are bridged by a pair of carboxylate groups into a dimer unit. Neighboring dimer units are further linked by tbip ligands to form a 2D helical layer in which the left and right helical chains appear alternatively by sharing the [Co_2(tbip)$_2$] binuclear nodes. One helix is formed by carboxylic oxygen atoms bridging Co1 and Co3 atoms, which is generated around the crystallographic 2_1 axis with a pitch of 13.4 Å. The other type of helix is built from carboxylic oxygen atom bridges between the Co2 centers, also with a pitch of 13.4 Å, but displaying the opposite helical orientation to the former helix (Figure 3b). Adjacent helical layers are connected by dpe pillars to generate a novel 3D open framework encapsulating

(19) (a) Fredericks, J. R.; Hamilton, A. D. Hydrogen Bonding Control of Molecular Self-Assembly: Recent Advances in Design, Synthesis and Analysis. In *Comprehensive Supramolecular Chemistry*; Sauvage, J. P., Hosseini, M. W., Eds.; Pergamon: Oxford, 1996; Vol. 9, chapter 16. (b) Lehn, J. M. *Science* **2002**, *295*, 2400. (c) Zhang, J.; Li, Z. J.; Kang, Y.; Cheng, J. K.; Yao, Y. G. *Inorg. Chem.* **2004**, *43*, 8085. (d) Ghosh, S. K.; Bharadwaj, P. K. *Eur. J. Inorg. Chem.* **2005**, 4886.

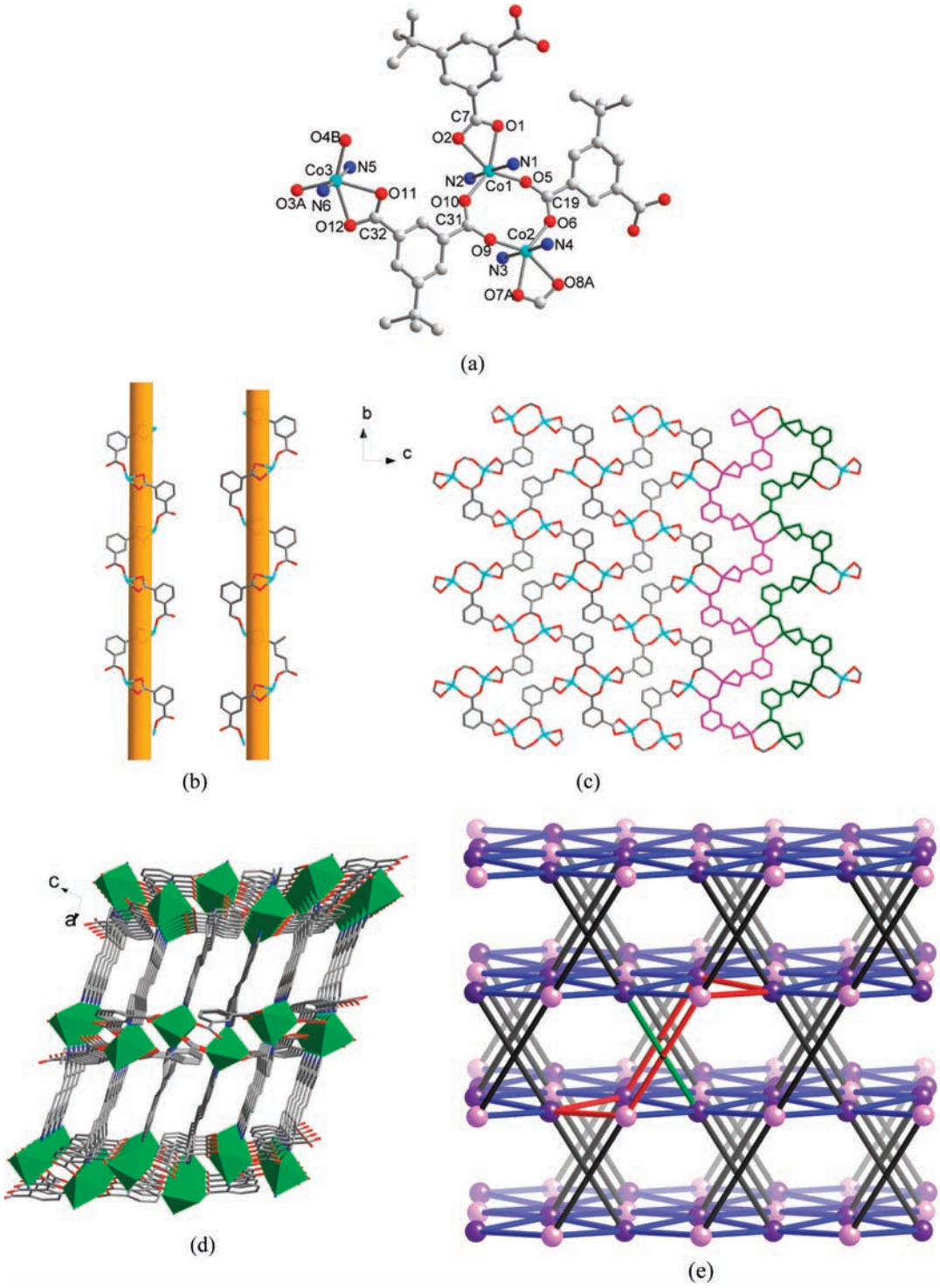

Figure 3. (a) Coordination environment of the trinuclear cobalt unit in **3**. (b) View of left- and right-handed helical chains. The *tert*-butyl groups are omitted for clarity. (c) View of a 2D layer constructed via the left-handed and right-handed helical chains. (d) Projection along the *b* axis of 3D framework in **3**. (e) The self-penetrating $4^8.6^6.8$ six-connected topology. Purple spheres represent the Co_2 dimer nodes (the lighter-shaded ones are the $(Co3)_2$ dimers). Blue bonds represent the tbip bridges, and black bonds represent the bridging dpe pairs. The passing of a rod through one of the six-membered shortest circuits is highlighted.

free dpe guest molecules (Figure 3d and Figure S1, Supporting Information). The effective free volume of **3** was calculated by PLATON analysis as 14.6% of the crystal volume (2135.1 out of the 14623.1 $Å^3$ unit cell volume).

Topologically, the Co dimers can be regarded as the network nodes. These are linked in two dimensions by the tbip ligands, to give (4,4) sheets, and in the third dimension by pairs of dpe ligands acting as single bridges. For each cluster, one pair of dpe ligands bridges to the sheet above, and another bridges to the sheet below, making the Co dimers

(20) He, H. Y.; Zhou, Y. L.; Hong, Y.; Zhu, L. G. *J. Mol. Struct.* **2005**, *737*, 97.

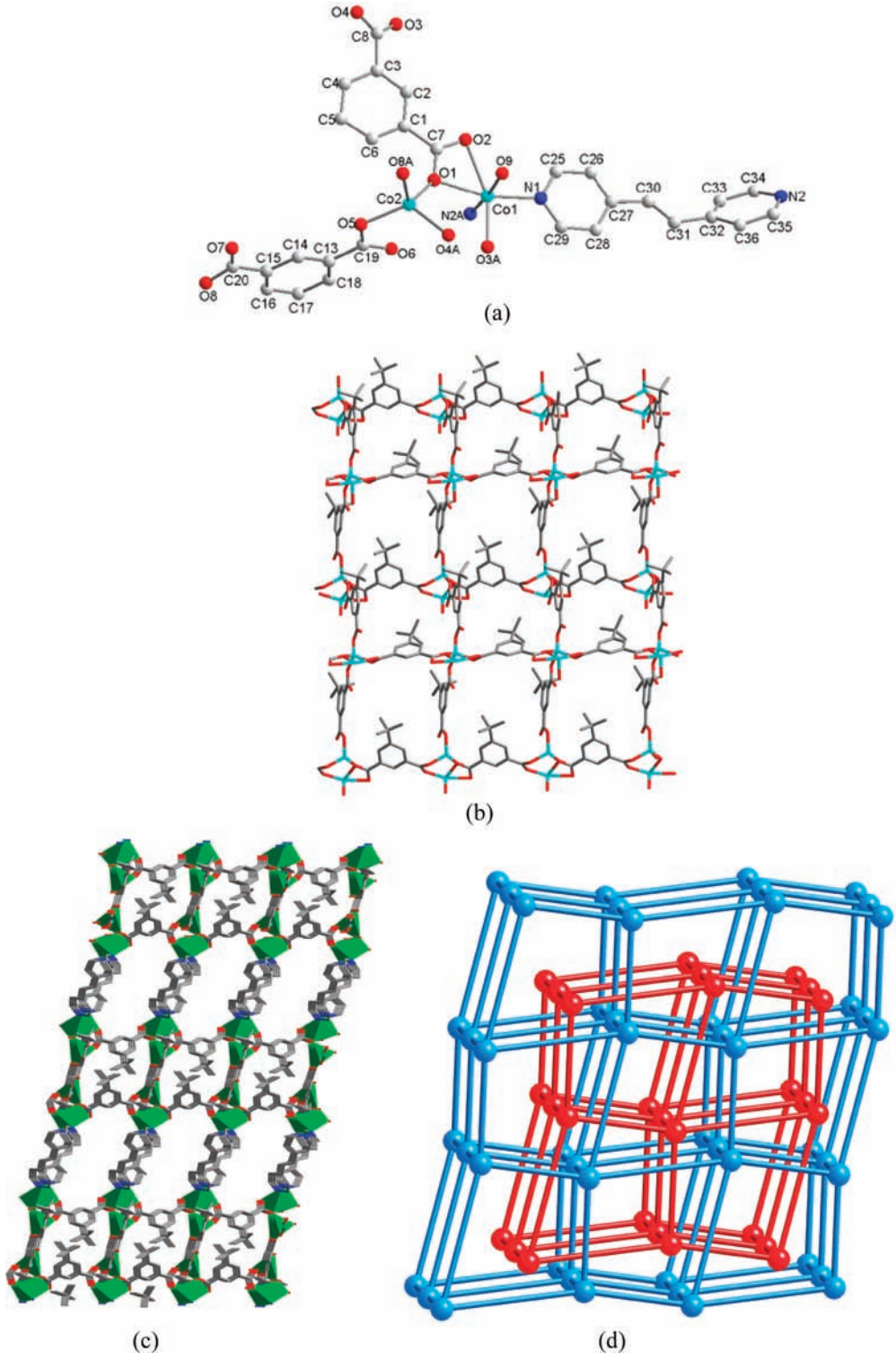

Figure 4. (a) Coordination environment of the dinuclear cobalt unit in **4**. The *tert*-butyl groups are ommitted for clarity. (b) The dinuclear cobalt clusters connected by H_2tbip ligands to form a 2D layer along *c* axis. (c) A polyhedral view of the 3D structure of **4** viewed along the *c* axis. (d) Schematic representation of the interpenetration; spheres represent the cobalt dimer nodes.

six-connecting nodes. The dpe bridges, however, are slanted rather than perpendicular to the sheets and crisscross in two different directions (Figure 3e). Thus, the usual α-Po net is not formed, but rather a more unusual uninodal six-connected net with $4^8.6^6.8$ topology is formed. This net is self-penetrating—that is, there are six-membered shortest circuits that are penetrated by rods of the same net. Self-penetration is an unusual form of topological entanglement,[21] although a number of related structures with self-penetrating networks constructed from (4,4) sheets connected by slanted bridges have been reported,[22] including some examples with the same topology as **3**.[22b,23]

$[Co_2(tbip)_2(dpe)(H_2O)]_n$ (4) and $[Co_2(tbip)_2(bpa)(H_2O)]_n$ (5). As listed in Table 1, compounds **4** and **5** crystallize in the same monoclinic form with space group $P2_1/n$ and have

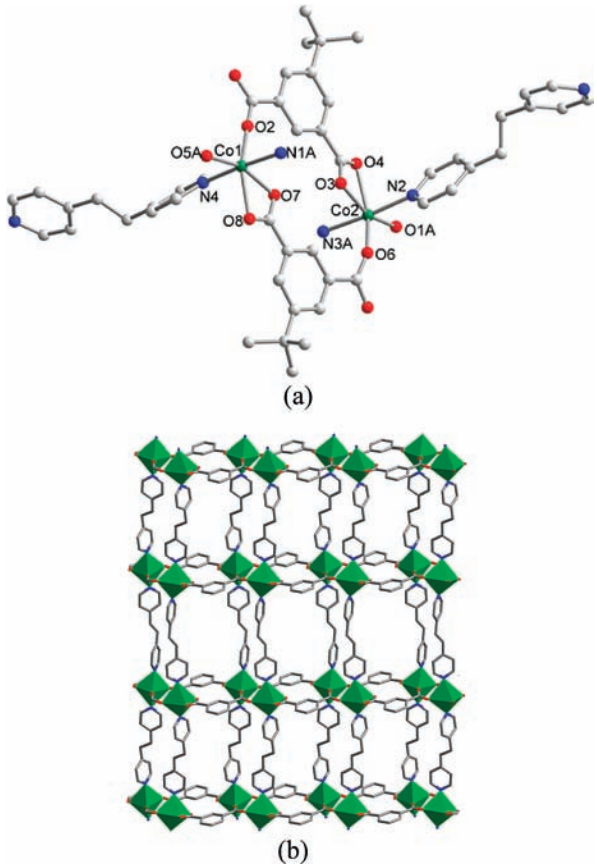

Figure 5. (a) Coordination environment of the dinuclear cobalt unit in **6**. (b) 1D chains pillared by flexible bpa ligands into a 2D layer.

similar cell parameters. The results of crystal structure analysis reveal that they are isostructural, and thus only the structure of **4** is described here as an example. The crystal structure of **4** exhibits a 3D network composed of the binuclear cobalt cluster nodes, dpe and tbip bridging ligands. There are two crystallographic independent cobalt atoms in compound **4** (Figure 4a). Co1 is six-coordinated and resides in a distorted octahedral [O_4N_2] coordination geometry. The six atoms coordinated to the Co1 ion come from two nitrogen atoms of two dpe ligands and three oxygen atoms from two tbip ligands, as well as one oxygen atom of a water molecule. The Co1−N distances are 2.1044(16) and 2.1457(16) Å, and the Co1−O distances are in the range of 2.0876(13)−2.3761(14) Å. Co2 adopts a distorted tetrahedral [O_4] coordination environment and is coordinated by four carboxylic oxygen atoms from four tbip ligands. The Co2−O bond distances are in the range of 1.9585(14)−1.9976(13) Å, which is shorter than those of the Co1−O bond lengths. In addition, tbip ligands exhibit two kinds of coordination modes, as shown in Scheme 1c and d. In the first mode, two carboxylate groups act as bis-monodentate ligands to bridge two Co atoms. In the second mode, two carboxylate groups act as pentadentate ligands to bridge four Co atoms together. On the basis of these connection modes, each binuclear Co cluster is linked to four neighboring clusters by four bridging tbip ligands, to form a 2D (4,4) layer parallel to the [110] direction, as shown in Figure 4b and Figure S2, Supporting Information. The 2D sheets are further connected by dpe ligands coordinating to the binuclear SBUs to form a 3D framework with six-connected α-Po topology, and two of these networks interpenetrate to generate the overall structure, as depicted in Figure S2 and Figure 4e.

Hydrothermal reactions of cobalt(II) salt with dpe and NO_2−BDC (NO_2−BDC = 5-nitro-1,3-benzenedicarboxylic acid) led to the formation of $\{Co(dpe)(NO_2-BDC)\}\cdot 0.5(dpe)]_n\cdot nH_2O$ (**9**) in the literature.[24] Compound **9** is a noninterpenetrated 2D bilayer with nanoscale rectangular channels that clathrate large organic molecules. This structure was obviously different from those of **3** and **4**, which further confirms the effect of the steric bulk of the bulky *tert*-butyl skeleton on the final structure.

$\{[Co_2(tbip)_2(bpa)_2]\cdot 2.5H_2O\}_n$ (6). As shown in Figure 5a, there are two crystallographic independent cobalt ions in **6**. Each Co(II) ion is coordinated by four oxygen atoms of three tbip anions and two nitrogen atoms of two bpa molecules. The coordination geometry can be described as a distorted octahedron. Two Co(II) ions are bridged by a pair of carboxylic groups from two different tbip anions into a binuclear Co unit with a Co···Co distance of 4.40 Å, which is larger than that in **2** (4.11 Å), revealing that the second ligand has a great influence on the 2D framework. The dimeric Co2 units are linked by two exotetradentate tbip anions to two adjacent dinuclear cobalt units, thus generating a 1D $[Co_2(tbip)_2]_n$ double chain (Figure S3, Supporting Information), in which the coordination modes of tbip anions are similar to those of **2**. All of the bpa ligands adopt an anti conformation and further link adjacent double chains into a 2D layer (Figure 5b). There are hydrogen bonds between the free water molecules and the coordinated carboxylic oxygen atoms (O9−H(1W)···O4, O···O = 2.991(12) Å, ∠OHO = 174.8°), which brings further stability for the structure. It is noteworthy that the 2D structure of **6** is similar to that of **2** except for the free water molecules. This comparison indicates that the 2D structure of **6** can be converted into the 2D layer of **2** through the replacement of the rigid bipy ligands by flexible bpa ligands.

PXRD and Thermal Analysis. In order to check the phase purity of these compounds, the PXRD patterns of compounds **1**−**6** were checked at room temperature. As shown in Figure S4, Supporting Information, the peak positions of the simulated and experimental PXRD patterns are in agreement with each other, demonstrating the good phase purity of the

(21) (a) Batten, S. R. *CrystEngComm* **2001**, *3*, 67. (b) Carlucci, L.; Ciani, G.; Proserpio, D. M. *Coord. Chem. Rev.* **2003**, *246*, 247. (c) Abrahams, B. F.; Batten, S. R.; Grannas, M. J.; Hamit, H.; Hoskins, B. F.; Robson, R. *Angew. Chem., Int. Ed.* **1999**, *38*, 1475. (d) Jensen, P.; Price, D. J.; Batten, S. R.; Moubaraki, B.; Murray, K. S. *Chem.—Eur. J.* **2000**, *6*, 3186. (e) Wang, X.-L.; Qin, C.; Wang, E.-B.; Su, Z.-M.; Xu, L.; Batten, S. R. *Chem. Commun.* **2005**, 4789. (f) Tong, M.-L.; Chen, X.-M.; Batten, S. R. *J. Am. Chem. Soc.* **2003**, *125*, 16170.

(22) (a) Sun, H.-L.; Gao, S.; Ma, B.-Q.; Batten, S. R. *CrystEngComm* **2004**, *6*, 579. (b) Abrahams, B. F.; Hardie, M. J.; Hoskins, B. F.; Robson, R.; Sutherland, E. E. *J. Chem. Soc., Chem. Commun.* **1994**, 1049.

(23) (a) Zhao, X. J.; Batten, S. R.; Du, M. *Acta Crystallogr., Sect. E* **2004**, *60*, m1237. (b) Long, D.-L.; Hill, R. J.; Blake, A. J.; Champness, N. R.; Hubberstey, P.; Wilson, C.; Schröder, M. *Chem.—Eur. J.* **2005**, *11*, 1384.

(24) Luo, J. H.; Hong, M. C.; Wang, R. H.; Cao, R.; Han, L.; Yuan, D. Q.; Lin, Z. Z.; Zhou, Y. F. *Inorg. Chem.* **2003**, *42*, 4486.

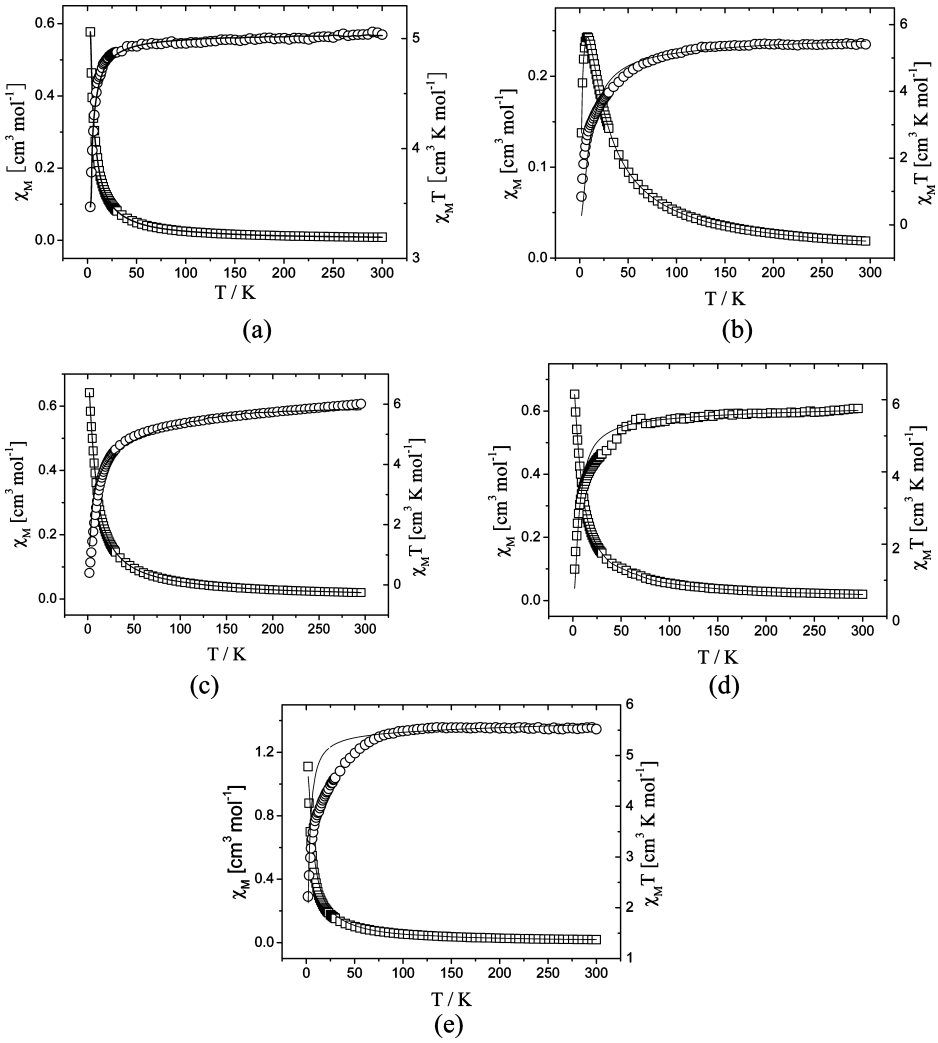

Figure 6. Temperature dependence of $\chi_M T$ and χ_M for **2** (a), **3** (b) **4** (c), **5** (d), and **6** (e). Open points are the experimental data, and the solid line represents the best fit obtained from the Hamiltonian given in the text.

compounds. The differences in intensity may be due to the preferred orientation of the crystalline powder samples.

Due to the presence of large amounts of solvent and guest molecules, thermogravimetric analysis (TGA) was performed on samples of complexes **1**, **3**, and **6** to confirm their stability, as shown in Figure S5, Supporting Information. The TG curve of complex **1** reveals a steady weight loss between 25 and 300 °C, which is attributed to the loss of lattice water molecules, coordinated water molecules, and free bipy molecules (observed, 23.74%, calculated, 25.58%). In **3**, the first event occurs between 25 and 285 °C, which corresponds to the loss of guest dpe and lattice water molecules (observed, 11.06%, calculated, 9.56%). And further weight loss was observed at a temperature of 650 °C. The TG curve for **6** shows an initial weight loss in the temperature range 25−120 °C, which was due to the loss of the lattice water molecules (observed, 3.8%, calculated, 4.6%). The further weight loss represents the decomposition of the material.

PXRD measurements at different temperatures show that, for complexes **3** and **6** after heating at 285 and 120 °C, the spectra are similar to the original ones, suggesting that their crystalline nature is still maintained after removing the solvent and guest dpe molecules. However, the crystalline nature of **1** largely decreased after heating at 300 °C.

Magnetic Properties. The magnetic susceptibilities, χ_M, of **2**−**6** were measured in the 2−300 K temperature range, and shown as $\chi_M T$ and χ_M versus T plots in Figure 6. As the temperature was lowered to 2 K, the $\chi_M T$ value continuously decreased, which suggests that antiferromagnetic interactions are operative in **2**−**6**. The experimental $\chi_M T$ values of **2**−**6** at room temperature are 5.40, 5.04, 5.81, 5.75, and 5.61 cm^3 K mol^{-1}, respectively, which are larger than two isolated spin-only Co^{2+} cations (3.75 cm^3 K mol^{-1}). This larger value is the result of contributions to the susceptibility from orbital angular momentum at high temperatures.[25a] The temperature dependence of the reciprocal susceptibilities ($1/\chi_M$) of **2**−**6** all obey the Curie−Weiss law above 50 K with $\theta = -19.34$ K, $C = 5.32$ cm^3·K/mol, and $R = 2.13 \times 10^{-3}$ for **2**; $\theta = -19.48$ K, $C = 5.52$ cm^3·K/mol, and $R = 1.47 \times 10^{-3}$ for **3**; $\theta = -28.87$ K, $C = 5.73$ cm^3·K/mol, and $R = 4.8 \times 10^{-4}$ for **4**; $\theta = -24.48$ K, $C = 5.86$ cm^3·K/mol, and $R = 4.22 \times 10^{-4}$ for **5**; and $\theta = -18.92$ K, $C = 5.37$ cm^3·K/mol, and $R = 3.14 \times 10^{-4}$ for **6**. The moderate negative θ values indicate the presence of antiferromagnetic interactions

among adjacent Co(II) ions even if a contribution from the spin−orbit coupling of Co(II) is also present.[25b,c] Comparable antiferromagnetic interactions between the Co(II) ions were reported in other cobalt compounds.[25]

According to the structural analyses of **2**−**6** discussed above, at least one Co(II) ion in each structure has octahedral geometry. It is well-known that the Co(II) ion in an octahedron possesses a $^4T_{1g}$ ground state, and thus the orbit angular momentum of the Co(II) ion will have a large contribution to the magnetic susceptibilities of these compounds. This implies that the magnetic analyses for Co-containing compounds will become rather complicated,[26] and some approximate methods are often applied to analyze magnetic interaction between Co ions. In this work, the main magnetic interactions may be considered to occur between adjacent Co(II) ions bridged by carboxylic groups and oxygen atoms, whereas the exchange interactions between Co(II) ions bridged through the tbip ligand and dpe or bpa can be ignored because of the long Co···Co separations. An attempt was made to fit the magnetic susceptibility data assuming that the carboxylic group bridges between Co(II) ions to form a binuclear unit with coupling constant J and then tbip and dpe or bpa connect the binuclear units to form a 3D network with an exchange constant zJ'. The susceptibility data were thus approximately analyzed by an isotropic dimer mode of spin $S = 3/2$.[27]

$$\chi_M = \frac{Ng^2\beta^2}{KT}\frac{A}{B} \quad (1)$$

$$A = 2\exp[-2J/KT] + 10\exp[-6J/KT] + 28\exp[-12J/KT]$$

$$B = 1 + 3\exp[-2J/KT] + 5\exp[-6J/KT] + 7\exp[-12J/KT]$$

The least-squares analysis of magnetic susceptibilities data led to $J = -0.83$ cm^{-1}, $g = 2.32$, $zJ' = -0.09$ cm^{-1}, and $R = 9.25 \times 10^{-5}$ for **2**; $J = -1.8$ cm^{-1}, $g = 2.41$, $zJ' = -0.47$ cm^{-1}, and $R = 3.96 \times 10^{-3}$ for **3**; $J = -1.5$ cm^{-1}, $g = 2.41$, $zJ' = -0.39$ cm^{-1}, and $R = 4.4 \times 10^{-3}$ for **4**; $J = -1.05$ cm^{-1}, $g = 2.45$, $zJ' = -0.21$ cm^{-1}, and $R = 2.5 \times 10^{-3}$ for **5**; and $J = -0.68$ cm^{-1}, $g = 2.38$, $zJ' = -0.08$ cm^{-1}, and $R = 3.16 \times 10^{-3}$ for **6**.

Conclusion

In summary, six novel Co(II) complexes have been synthesized by the self-assembly of Co(II) salts with H_2tbip and dipyridyl-based ligands. Assemblies of these complexes generate four types of diverse frameworks: a 1D chain, two 2D layers, one 3D self-penetrating $4^8.6^6.8$ framework, and two 2-fold interpenetrating 3D α-Po networks. We have found that the presence of bulky electron-donating ($-C(CH_3)_3$) noncoordinating groups in dicarboxylate ligands is very helpful for the construction of metal-organic frameworks. Compound **3** has a stable metal-organic framework subject to the loss of guest molecules. In addition, the magnetic properties for **2**−**6** have been investigated, along with the corresponding J parameter related to their structural characteristics. Subsequent works will be focused on the construction of novel coordination polymers by reacting these and other related ligands with more metal ions.

Acknowledgment. This work was supported by the Natural Science Foundation of China (nos. 20471026 and 20771054), the Henan tackle key problem of science and technology (nos. 072102270030 and 072102270034), and the Foundation of Education Committee of Henan province (nos. 2006150017 and 2008A150018).

Supporting Information Available: Crystallographic data in CIF format and additional figures, selected bond distances and angles, and patterns of TGA and PXRD in PDF format. This information is available free of charge via the Internet at http://pubs.acs.org.

IC801278J

(25) (a) Xu, Y. Q.; Yuan, D. Q.; Wu, B. L.; Han, L.; Wu, M. Y.; Jiang, F. L.; Hong, M. C. *Cryst. Growth Des.* **2006**, *6*, 1168. (b) Bourne, S. A.; Lu, J. J.; Mondal, A.; Moulton, B.; Zaworotko, M. J. *Angew. Chem., Int. Ed.* **2001**, *40*, 2111. (c) Luo, J. H.; Zhao, Y. S.; Xu, H. W.; Kinnibrugh, T. L.; Yang, D.; Timofeeva, T. V.; Daemen, L. L.; Zhang, J. Z.; Bao, W.; Thompson, J. D.; Currier, R. P. *Inorg. Chem.* **2007**, *46*, 9021. (d) Sakiyama, H.; Tto, R.; Kumagai, H.; Inoue, K.; Sakamoto, M.; Nishida, Y.; Yamasaki, M. *Eur. J. Inorg. Chem.* **2001**, 2027. (e) Wang, Y. L.; Yuan, D. Q.; Bi, W. H.; Li, X.; Li, X. J.; Li, F.; Cao, R. *Cryst. Growth. Des.* **2005**, *5*, 1849. (f) Blake, A. B. *J. Chem. Soc., Chem. Commun.* **1966**, 569.

(26) Fabelo, O.; Pasán, J.; Cañadillas-Delgado, L.; Delgado, F. S.; Lloret, F.; Julve, M.; Ruiz-Pérez, C. *Inorg. Chem.* **2008**, [Online] DOI: 10.1021/ic800704y.

(27) Connor, C. J. O. *Prog. Inorg. Chem.* **1982**, *29*, 203.